Quaternary International xxx (2016) 1–13

Contents lists available at ScienceDirect

Quaternary International

journal homepage: www.elsevier.com/locate/quaint

# Numerical approach to the study of coastal boulders: The case of Martigues, Marseille, France

A. Piscitelli [a], M. Milella [a], J.-C. Hippolyte [b], M. Shah-Hosseini [b], C. Morhange [b], G. Mastronuzzi [c, *]

[a] Spin Off Environmental Surveys s.r.l., Taranto, Italy
[b] Aix Marseille Université, CEREGE, UMR 7330, Technopôle Méditerranéenne l'Arbois, Aix en Provence, France
[c] Dipartimento di Scienze della Terra e Geoambientali, Università degli Studi di Bari "Aldo Moro", Bari, Italy

ARTICLE INFO

*Article history:*
Received 26 January 2016
Accepted 18 October 2016
Available online xxx

*Keywords:*
Sea storm
Boulders
Hydrodynamic equation

ABSTRACT

The coastal area extending east of the city of Martigues, between the bays of Bonnieu and that of Chariot, is characterized by an alternation of gently sloping rocky coast and 5 m high cliffs composed of Miocene limestone. The foot of the cliff is marked by a well developed notch and a discontinuous wave-cut platform; at its base, the sea bottom reaches a maximum depth of about 4.5–6 m. The emerged area shows boulders placed up to 10 m inland of the coastline at around 2 m above s.l. and, weighing as much as 35 tonnes. A geomorphological survey was conducted by means of a Terrestrial Laser Scanner to estimate boulder sizes. The particular focus of the proposed study was to estimate the minimum wave height required to detach and transport two boulders, originally joined together as one bigger one and weighing approximately 25 tonnes, from the wave-cut platform onto the surf bench. Hydrodynamic models developed by various authors were used to calculate the minimum wave height necessary to move them. The data obtained from the resulting hydrodynamic equations were compared to wave-climate data collected over the last 15 years by the buoy off the coast of Marseille, in the Gulf of Lion. The present study seems to confirm that it would not have been necessary to have a tsunami impact (among other things, never recorded in the last 20 years) to move a 25 tonnes boulder. Indeed, hydrodynamic equations suggest that the boulder might have been broken and only subsequently moved due to the impact of waves generated by an extreme storm which would have occurred prior to December 2003. This hypothesis seems to be in agreement with the morphology of the sea bottom, hydrodynamic features of the area as well as eyewitnesses.



## 1. Introduction

In recent years, scientific debate on coastal dynamics has focused also on the effects of extreme wave impact on coastal areas, thus increasing the awareness of the high risks these impacts pose on all human settlements as well as on the environment. Indeed, examples of hurricane impacts which have occurred in the last fifteen years, inducing exceptional waves and devastating tsunamis, underline the fact that morphological effects cannot be underestimated neither in purely scientific terms nor in application to the Integrated Coastal Zone Management (ICZM) (i.e.: Mastronuzzi et al., 2013). In particular, an important field of science dealing with coastal morphodynamics studies large boulder accumulations distributed along the coastline of the Mediterranean basin as an attempt to reconstruct the sequence of the high energy event that distribute boulders along the coast using historical or chronological data (i.e.: Mastronuzzi and Sansò, 2000, 2004; Morhange et al., 2006; Mastronuzzi et al., 2006, 2007; Scicchitano et al., 2007; Maouche et al., 2009; Vött et al., 2010; Mastronuzzi and Pignatelli, 2012; Shah-Hosseini et al., 2013; Anzidei et al., 2014; Biolchi et al., 2016). The study of extreme waves impacting all along the coasts of the world over the past 25 years suggested that boulder accumulations are the consequence of impacts of both storm surges and tsunamis (Mastronuzzi and Sansò, 2004; Goto et al., 2007; Barbano et al., 2010; Bourgeois and MacInnes, 2010; Regnauld et al., 2010; Paris et al., 2010; Richmond et al., 2011;

* Corresponding author. Dipartimento di Scienze della Terra e Geoambientali, Università degli Studi di Bari "Aldo Moro", Campus Universitario, Via E. Orabona 4, 70125 Bari, Italy.
*E-mail addresses:* giuseppeantonio.mastronuzzi@uniba.it, gimastronuzzi@libero.it (G. Mastronuzzi).

http://dx.doi.org/10.1016/j.quaint.2016.10.042
1040-6182/

Jaffe et al., 2011, 2012). Unfortunately, a method by which it is possible to unequivocally identify the nature of the impact has yet to be found. Using the sizes and shapes of boulders surveyed along the coast, many authors developed hydrodynamic equations to build a model able to recognize the origin of their deposits (Nott, 2003; Noormets et al., 2004; Imamura et al., 2008; Pignatelli et al., 2009; Nandasena et al., 2011; Benner et al., 2010; Engel and May 2012). These hydrodynamic equations have been widely used by various authors to investigate the origin of past boulder accumulations in many coastal areas of the Mediterranean basin (i.e.: Mastronuzzi and Sansò, 2004; Shah-Hosseini et al., 2013; Biolchi et al., 2016).

In particular, the rocky Mediterranean coast of Southern France, along the coastal area of Martigues, near Marseilles (Fig. 1), is characterized by the presence of large boulders placed at various distances from the coastline and and elevations above sea level, thus, testifying the impact of exceptional wave(s) that scattered boulders from the midtidal and subtidal zones (Vella et al., 2011) inland. The origin of the extreme events responsible for their transport and accumulation remains unclear, even though a series of surveys conducted, using classic, modern and even digital techniques (Shah-Hosseini et al., 2013) have attributed them to exceptional storms that occurred during the Little Ice Age (LIA). Nevertheless, the possibility that multiple events, including a tsunami, may have been the cause cannot be ruled out. Particular focus was placed on two boulders, "A" and "B", indicated by the local inhabitants as originating from a single one, "C".

In a previous paper, Shah-Hosseini et al. (2013) using the large presence of bio-encrustations as bio-indicators, reconstructed the four phases of the breaking and the transport of the initial boulder ("C" in this paper, but M7 in the original one): ì - detachment of the original boulder from its initial intertidal position; íì - a submersion phase, attested by the development of Vermetids on the Lithophyllum bissoides encrustation; îì - breakdown into boulders, M5 (= "B") and M6 (="A") followed by the overturning of the latter; ìv - transport of the block to the supratidal zone. With the main aim to confirm this geomorphological model by means of a digital and mathematical approach, a detailed laser scan survey of the two boulders and of the local topography was carried out together with a bathymetric survey of the coastal area right next to them. This allowed us to: ì –accurately reconstruct the present size of the boulders building their digital model; íì - reconstruct their original shape; îì – test the wave hydrodynamic equations developed by various authors to test their validity in a case study where the impacting wave is known to have been caused by a storm; ìv - reconstruct the sequence of events responsible for the breaking, transporting and depositing of the boulders.

## 2. Geographical, geological and wave climate settings

The present study was performed in an area located between the Bay of Bonnieu and that of Chariot, South of Martigues, near Marseilles, along the Mediterranean coast of France (Fig. 1). The coastal area is oriented northwest-southeast, and is characterized by a gently sloping rocky surface shaped in highly fractured bioclastic limestone. This Burdigalian marine limestone (Colomb et al., 1975) is characterized by bioclastic and pinkish conglomeratic calcarenite with *Chlamys*, *Ostrea* and *Pecten*, about 10 m thick overlying in discordance on Cretaceous (Urgonian) limestone. The outcrop is dense with faults and fractures presenting rough stratigraphic joints separating 50 cm to 2 m thick layers. Limestone beds gently dip to the southwest (<10°). Despite a lack of apparent finite

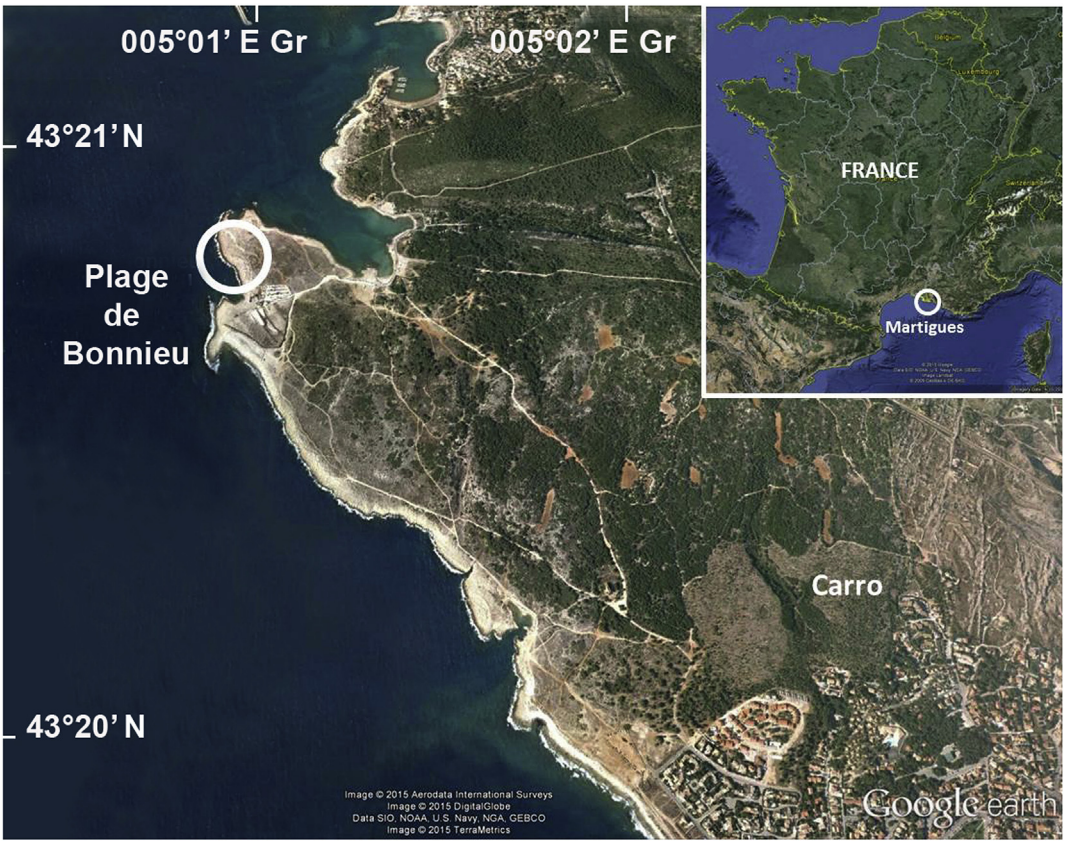


**Fig. 1.** Geographical position of the studied area (from Google Earth).

Please cite this article in press as: Piscitelli, A., et al., Numerical approach to the study of coastal boulders: The case of Martigues, Marseille, France, Quaternary International (2016), http://dx.doi.org/10.1016/j.quaint.2016.10.042

deformation, this limestone is cut by well-defined sets of fractures (Figs. 2 and 3). The fracture surfaces do not show evidence of shear displacement; hence, they can be referred to as joints. These joints are predominantly perpendicular to the bedding (Fig. 2A and B) and, together with the bedding joints, cut the limestone into blocks with planar surfaces. Near the sea shore, beneath the water, the

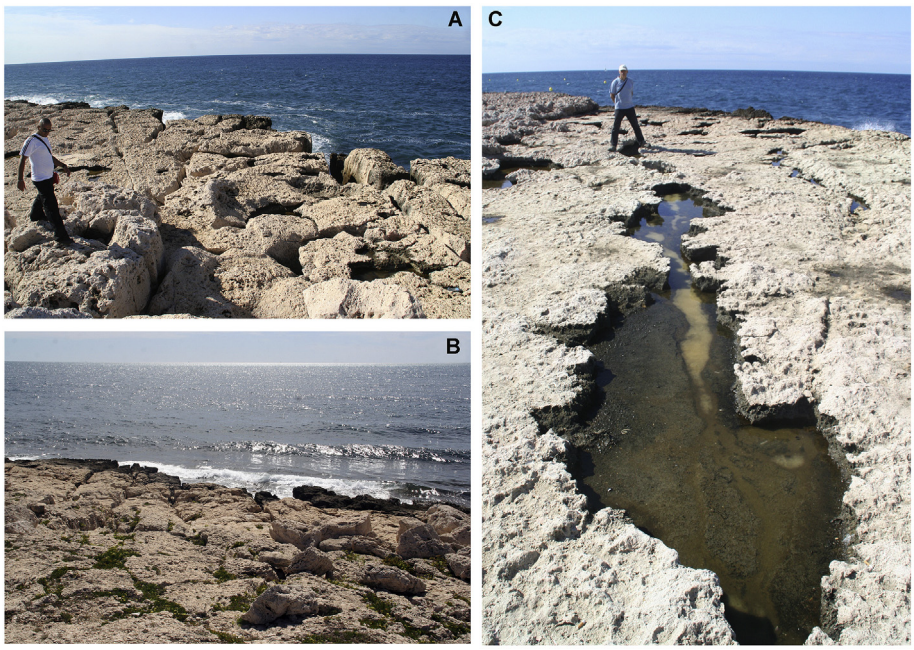


**Fig. 2.** Examples of fracture lines in the studied area; for A, B and C, see the text.

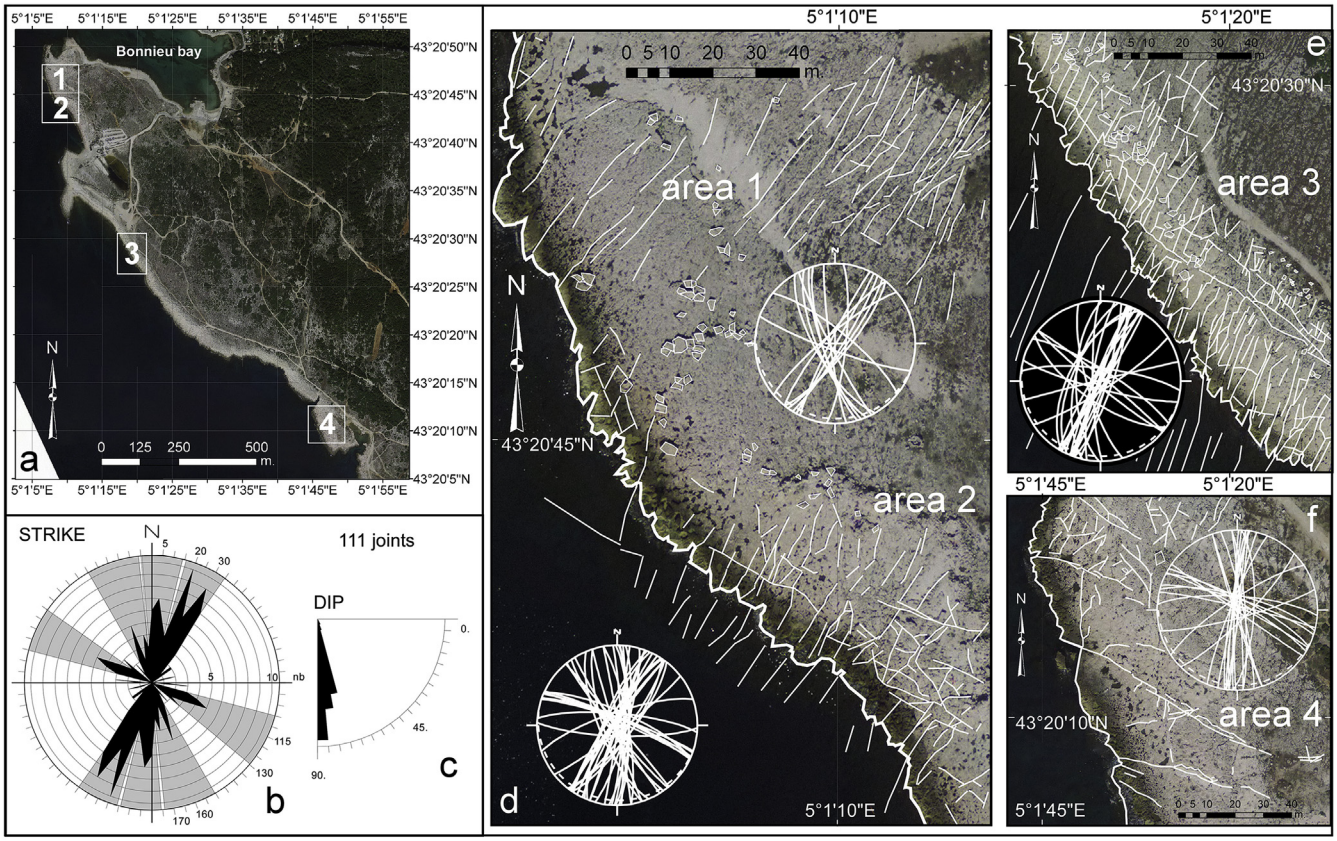


**Fig. 3.** Joint patterns along the coast between the Plage de Bonnieu and Charrot. a) Joints were surveyed and mapped in four areas. b) Rose diagram of the strike of the 111 measured joints. c) dip of the 111 measured joints. d, e, f) aerial photos with mapped joint patterns and boulders of areas 1 to 4. Schmidt nets (lower hemisphere) show the joint planes measured in each area.

Please cite this article in press as: Piscitelli, A., et al., Numerical approach to the study of coastal boulders: The case of Martigues, Marseille, France, Quaternary International (2016), http://dx.doi.org/10.1016/j.quaint.2016.10.042

joints are widely open as a result of dissolution and abrasion of the limestone (Fig. 2C). The coastal landscape shaping was conditioned by both the presence of these joints as well as sea action; the result is an alternation of surf benches, wave-cut platforms, and cliffs up to roughly 5 m high (Fig. 4).

The surf bench (hereinafter SB) generally corresponds to an area directly flooded by broken waves that have stripped off the soil and the upper strata of the local stratigraphic sequence; inland, it is delimited by a step having a height which corresponds to the strata thickness (Fig. 4A and B). In a small number of areas, a wave-cut platform (hereinafter WCP) of varying extension is shaped in continuity with the SB from which it is separated by a very low step, not higher than 1 m. Locally, a short WCP corresponding to the strata surface is also present at the base of the cliffs, which, in turn, are engraved by a continuous notch up to about 2 m deep and 1 m high (Fig. 4C and D). The emerged area is marked by the presence of hundreds of large boulders with a maximum size of about 35 tonnes, placed up to 10 m from the coastline and at about 2 m above sea level (Figs. 3 and 4A) (Vella et al., 2011; Shah-Hosseini et al., 2013).

The French Mediterranean basin is considered to have been a moderately active tectonic zone during the Holocene (Vella et al., 1998; Vella and Provansal, 2000; Jolivet et al., 2008). Rarely earthquakes that generates tsunamis have been reported (*Bureau de Recherches Géologiques et Miniéres* – BRGM, www.ngdc.noaa.gov). Archives report 14 tsunamis since 1755, with one destructive event occurring on 27th June 1812 (4 on the Sieberg-Ambraseys intensity scale), which damaged boats and infrastructures in the old port of Marseilles. The event may have been recorded in the accumulated boulders in the area of Martigues; indeed, 14C ages obtained on some bio-encrustations from a number of boulders seem to suggest a sequence of various high-energy wave impacts distributed over the past 700 years (Vella et al., 2011; Shah-Hosseini et al., 2013). Some 14C ages seem to fit in a period that comprises the 1812 event; on the other hand, the obtained ages range from 1660 to 1860, in a period corresponding to the LIA during which important storm events able to scrape and move boulders inland likely occurred (i.e.: Kaniewski et al., 2016; for the Central Mediterranean zone). Minor tsunami events have been recorded in historic and modern times on the French Riviera coast about 150 km east of Martigues. They were probably triggered by submarine landslides, but no geomorphological evidence has been found (Julian and Anthony, 1996).

Based on present knowledge, there is no evidence that leads to a correlation between the surveyed boulders and the impact of a tsunami, as opposed to that of a storm. However, it is also possible that storms characterising this stretch of coast, due to their energy, may be able to move large boulders.

The surveyed coast is exposed to S-NW winds and the fetch is between 400 to about 600 nautical miles, even if protected by the Balearic Islands. Available wave data sets on the French Mediterranean coast are of short durations. These data derive from the buoy placed in the Gulf of Lion, France (Fig. 5). The data collected, for a total of 1534 events, record wave heights, period and direction only for waves with heights > 3 m, in the period 1993–2008 (Table 1). Table 2 shows the highest waves and their provenance direction, recorded by the buoy in the same period for each year.

## 3. Material and methods

A geomorphological and structural survey was conducted along the entire coastal area of Carro, where boulders have been detected (Vella et al., 2011; Shah-Hosseini et al., 2013). In order to characterise the structural features of the area, joint planes have been measured in four areas directly in-field (Fig. 3). The survey focused on a restricted portion (25 m × 25 m) of the coastal area containing two boulders, hereinafter named “A” and “B”. The detailed terrestrial laser scan (TLS) survey of this area was carried out using a Leica Scan Station 2 operated jointly with a digital ground position system (DGPS) Leica 1230 (Fig. 6).

The scanner consists of a laser beam generator, a mirror rotating on its horizontal axis and forming a 45° degree angle with the beam direction simultaneously rotating around its vertical axis. Together, these features allow to obtain a scan of an area extending 360° × 270°.

To obtain a complete coverage of the surveyed area, a scan


**Fig. 4.** Morphological features of the studied area. A: gently sloping rocky coast characterized by boulder accumulation and soil cover; B: boulder field in the surveyed area; C: cliff about 4 m high; D: notch at the foot of the cliff.

Please cite this article in press as: Piscitelli, A., et al., Numerical approach to the study of coastal boulders: The case of Martigues, Marseille, France, Quaternary International (2016), http://dx.doi.org/10.1016/j.quaint.2016.10.042

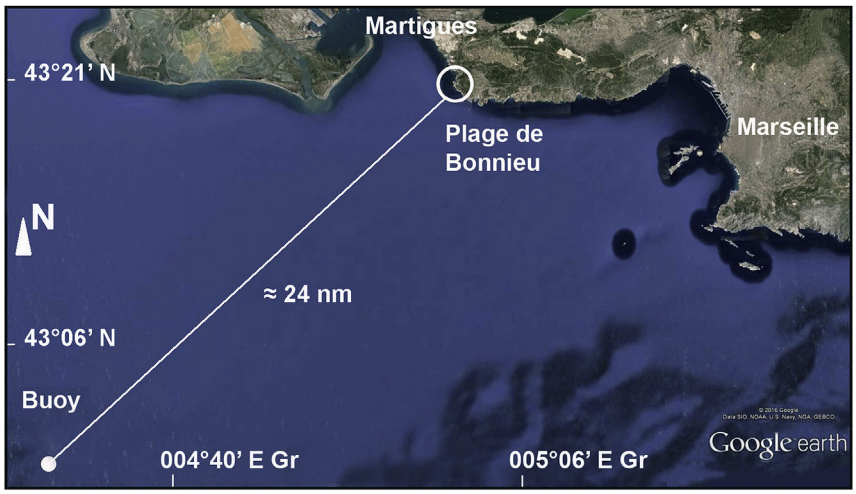


**Fig. 5.** Position of the buoy in the Gulf of Lion (from Google Earth).

**Table 1**
Number of events >3 m high, per year, recorded by the buoy in the period 1993–2008.

| Year | Number of Waves with Height H > 3 m | | | | |
|---|---|---|---|---|---|
| | I Sector | II Sector | III Sector | IV Sector | Total |
| 1993 | 21 | 9 | 0 | 31 | **61** |
| 1994 | 1 | 20 | 12 | 23 | **56** |
| 1995 | 1 | 43 | 5 | 43 | **92** |
| 1996 | 16 | 93 | 12 | 15 | **136** |
| 1997 | 6 | 39 | 10 | 7 | **62** |
| 1998 | 8 | 6 | 1 | 20 | **35** |
| 1999 | 0 | 19 | 17 | 33 | **69** |
| 2000 | 14 | 27 | 13 | 14 | **68** |
| 2001 | 22 | 15 | 15 | 9 | **61** |
| 2002 | 12 | 49 | 10 | 7 | **78** |
| 2003 | 7 | 78 | 8 | 29 | **122** |
| 2004 | 3 | 50 | 6 | 29 | **88** |
| 2005 | 27 | 33 | 7 | 81 | **148** |
| 2006 | 10 | 30 | 18 | 21 | **79** |
| 2007 | 48 | 41 | 0 | 108 | **197** |
| 2008 | 14 | 58 | 21 | 89 | **182** |
| **TOTAL** | **210** | **610** | **155** | **559** | **1534** |

**Table 2**
Highest waves recorded by the buoy, for each year, in the period 1993–2008. H: height of wave in m; °N: wave direction.

| Year | Highest Wave (m) per Directions | | | |
|---|---|---|---|---|
| | I Sector H - °N | II Sector H - °N | III Sector H - °N | IV Sector H - °N |
| 1993 | 4,16–88° | 3,57–91° | // | 4,19–318° |
| 1994 | 3,22–88° | 4,29–98° | 4,87–188° | 3,94–320° |
| 1995 | 4,32–90° | 4,34–91° | 3,77–187° | 4,02–303° |
| 1996 | 3,99–86° | 4,57–146° | 5,16–190° | 4,26–307° |
| 1997 | 3,98–89° | 6,08–96° | 5,07–187° | 3,30–325° |
| 1998 | 3,95–90° | 3,72–126° | 3,13–189° | 3,78–314° |
| 1999 | // | 5,24–97° | 4,03–199° | 4,07–294° |
| 2000 | 3,83–90° | 4,97–108° | 4,07–198° | 3,62–343° |
| 2001 | 4,62–88° | 4,60–91° | 4,66–203° | 3,50–323° |
| 2002 | 4,33–87° | 4,89–96° | 3,55–195° | 3,80–317° |
| 2003 | 3,86–90° | 6,47–107° | 5,25–202° | 3,77–352° |
| 2004 | 3,79–1° | 5,41–95° | 3,26–191° | 4,17–357° |
| 2005 | 3,85–4° | 3,54–105° | 5,15–200° | 4,20–314° |
| 2006 | 3,74–14° | 5,66–115° | 4,30–197° | 4,13–330° |
| 2007 | 4,31–3° | 4,95–97° | // | 4,34–296° |
| 2008 | 5,17–90° | 6,85–97° | 4,51–195° | 4,19–300° |

density of 3 mm was carried out from varying positions along the horizontal and vertical planes; different surveys were joined and overlapped using targets to geo-reference all the points scanned from different positions to obtain a 3D reconstruction of the surveyed objects included in "point clouds". Therefore, to obtain a 3D modelspace, it is necessary to overlap numerous scans in which targets were captured by means of a DGPS from different points of view. The post-processing was performed using Cyclone 6.03 software; the point clouds obtained from each scan were linked together via the overlapping of a number of TLS scans. The next step was to isolate millions of points representing boulders "A" and "B" from the cloud points that comprise all the landscape, and reconstruct the original boulder "C" by matching them along the fracture surface. The use of TLS techniques significantly reduces the overestimation of the sizes and weight of the surveyed boulders compared to handmade measurements; obviously, this allows the hydrodynamic equations to be used with greater confidence (Marsico et al., 2009; Hoffmeister et al., 2014).

In order to complete the sub-aerial survey in the "A" and "B" boulder area, a specific bathymetric survey was performed during both ARA and snorkelling dives. Indeed, nine different bathymetric transects were drawn starting from the biological mean sea level up to a 6 m bathymetry; depths and immersion times were recorded using the scuba computer SCUBAPRO Aladin 2G. This methodology enabled the reconstruction of a 3D sketch of the continuity morphology of both the emerged coastal area as well as the seabed up to about 50 m from the coastline (Fig. 7).

## 4. Coastal and boulders features

The rose diagram of the 111 measured joints shows the prevalence of two main trends: NNW-SSE to NNE-SSW and ESE-WNW (Fig. 3b). In detail, seven joint sets can be distinguished from this rose diagram: N160E, N170E, N5E, N20E, N30E, N115E and N130E (Fig. 3b). Taking into account that the Marseilles area underwent N020E and N165E compressions during the Miocene (Hippolyte et al., 1993) the NNW- to NNE-trending joints can be interpreted as tension or shear joints formed during the alpine compressional phases (late Cenozoic). On the contrary, the ESE-trending joints are filled with Miocene shells and sand suggesting early formation (Burdigalian).

Schmidt diagrams of joints (Fig. 3d, e, f) show that the four studied areas are characterized by at least two perpendicular joint sets which allowed the separation of limestone blocks (NNE-SSW

Please cite this article in press as: Piscitelli, A., et al., Numerical approach to the study of coastal boulders: The case of Martigues, Marseille, France, Quaternary International (2016), http://dx.doi.org/10.1016/j.quaint.2016.10.042

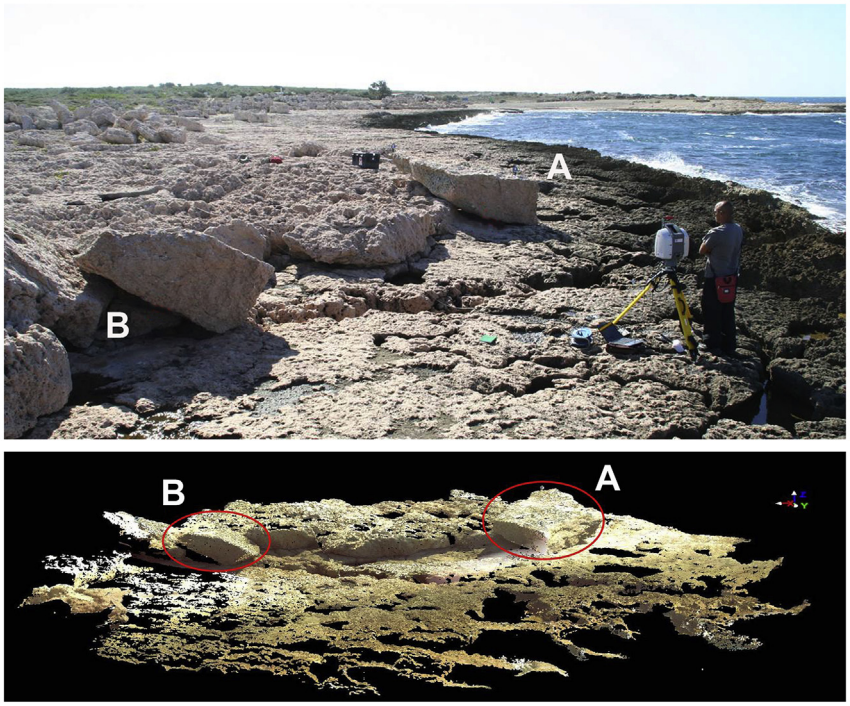


**Fig. 6.** Scanned area (above) and point cloud surveyed by TLS Leica Scanstation2 (below).

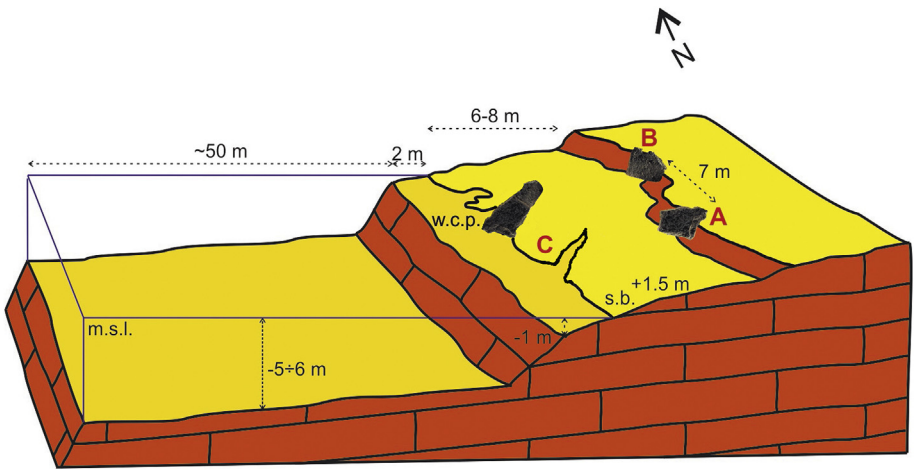


**Fig. 7.** Schematic sketch of the surveyed area. w.c.p. = wave-cut platform; s.b. = surf bench. Boulder "C" is located in the probable detachment area.

and ESE-WNW). We mapped the joint sets in the four areas along the coast using high resolution (15 cm) aerial photos (Fig. 3). Areas 1 to 3 show closely spaced NNE-trending joints and by numerous transported blocks (Fig. 3d and e). In contrast, area 4 presented far fewer NNE-trending joints and transported blocks. The dense joint patterns in areas 1 to 3 probably facilitated the rock detachment. As previously indicated, the coastal area shaping has been driven by sea action on a lithological sequence heavily conditioned by the presence of these joints. Surf benches, wave-cut platforms and cliffs alternate between Carro and Bonnieu (Fig. 4). The first 50 m of the sea bottom reach a maximum depth ranging from 4 to 6 m. In general, the surveyed area shows a double trend: from the coastline up to a depth of about 1.5 m it has quite a flat surface of varying extension corresponding to the wave-cut platform; a rapid increase of the slope up to 5–6 m deep indicates the passage to a gently sloping surface towards the higher depths.

Generally, boulders are distributed along the surf bench; at about 2 m above sea level, boulders "A" and "B" are 7 m apart, positioned on the SB, slightly leaning against a step whose height corresponds to the strata thickness (Fig. 4b). The details characterising the geometric features of all three boulders were obtained from the scanned point clouds, allowing an approximation within a few centimetres. The software used enabled the reconstruction of boulder "C" via the virtual rotation and shift of the "A" and "B" boulders (Fig. 8). All the geometrical parameters of boulders "A", "B" and "C" were obtained by laser scanner software, given the highly irregular shape of both blocks. The measurements of three axes, the planar a (maximum) and b (medium) ones, and the vertical c-axis, together with the volumes and weights are reported in the synoptic Table 3.

Please cite this article in press as: Piscitelli, A., et al., Numerical approach to the study of coastal boulders: The case of Martigues, Marseille, France, Quaternary International (2016), http://dx.doi.org/10.1016/j.quaint.2016.10.042

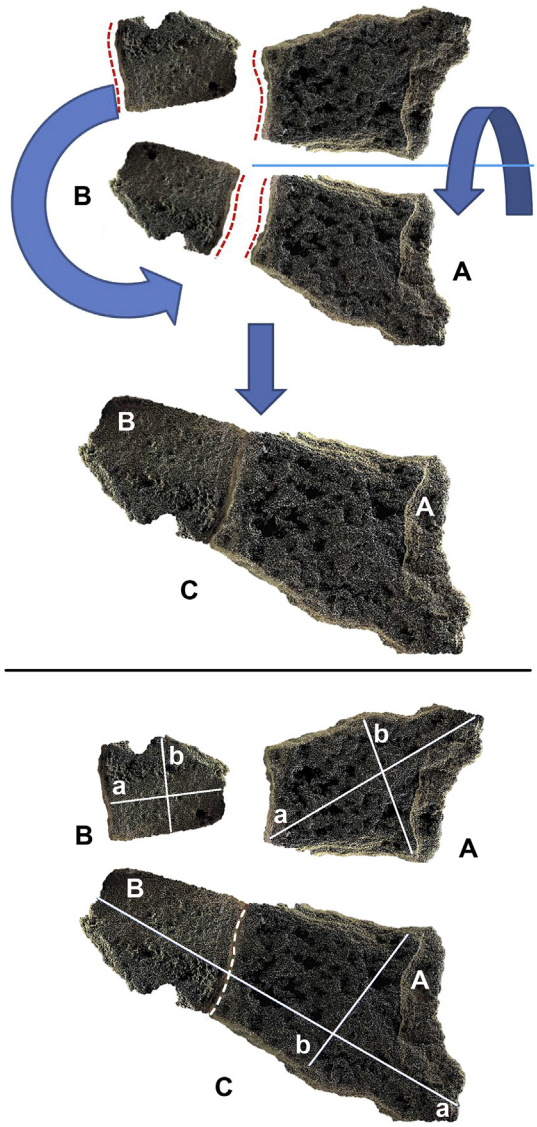


**Fig. 8.** Schematic reconstruction of the reverse procedure adopted to reconstruct the boulder "C" (above): the part "A" rolled-over, while the part "B" rotated. The red dotted lines represent the break surfaces. Boulders "A", "B" and "C" with their "a" and "b" axes (below); the white dotted line represents the break surface of the boulder "C". (For interpretation of the references to colour in this figure legend, the reader is referred to the web version of this article.)

Both boulders (Fig. 9a and b) show bio-encrustations typical of the midtidal zone base represented by the *Lithophyllum byssoides* rim, algae characterising the lowest limit of the biological sea level (Laborel and Laborel-Deguen, 1994; Morhange and Marriner, 2015). However, boulder "A", in particular, shows a side characterized by the presence of a concavity that seems to correspond to an abrasive surface originally placed in correspondence to the mean sea level. This geomorphological element confirms the initial position of boulder "C" in relation to the mean sea level.

The cover of the carbonate algae appears partially colonized by *Vermetus triqueter*; this gastropod develops in subtidal zones and the upper limit of the population which approximately marks the biological sea level (Laborel and Laborel-Deguen, 1994). Its presence, together with some specimens of *Lithophaga lithophaga* suggests a lowering of the original position of boulder "C". Finally, the presence of *Barnacles* sp. can be related to the permanence of the boulder in the surfing area. Boulder "A" is overturned compared to the original verticality of boulder "C" as confirmed both by the morphological evidence as well as the presence of the *L. byssoides* rim on its lower face. Furthermore, the rim indicates, with absolute approximation, the boulder's past interface with the mean biological sea level. On the other hand, boulder "B" is rotated, compared to the supposed original position of boulder "C"; this is evidenced by the particular aspect of the breaking surface that faces west (Fig. 9A–D), and is in the opposite direction of boulder "A". Boulder "B" is in the natural polarity as evidenced by the presence of the *L. byssoides* rim on its upper surface corresponding to the ancient surface below sea level.

The joint geomorphological and laser scan survey of the entire coastal area emphasized the presence of two fracture systems (Figs. 2 and 3). Moreover, considering the general structural features, and according to them, the first one is oriented NE-SW, almost perpendicular to the coastline, while the second is oriented WNW-ESE, quite parallel to the coastline. These two alignments and the general one of the coastline allowed us to hypothesize the original position and orientation of boulder "C", as well as identify the detachment zone, located on the WCP about 12 m south of the present position of boulder "B", between two evident fracture lines (Fig. 10).

## 5. Discussion

### 5.1. Reconstruction of the boulder's movement

The set of morphological and biological data and the bathymetric survey suggest a first reconstruction of the possible succession of the dynamic events that drove the two separated boulders to their current position on the rocky surface. This was made possible also by taking into account the virtual reconstruction of boulder "C" obtained by the TLS survey.

The general shape of the latter and the presence of a quite continuous concavity along one of its sides indicate an original position in relation to the mean sea level at the external sea side border of the surf bench. The extensive presence of *L. bissoides* on the top of boulders "A" – currently overturned - and "B" suggests that boulder "C" collapsed due to numerous and repeated wave impacts, ultimately depositing on the WCP, and, in the end, below sea level. As there is no evidence of marine organism colonies on its fracture surface, it did not break here. Only at a later time, after colonization by vermetids, did boulder "C" break into two blocks, "A" and "B", without their having been time for marine organisms to colonize the fracture before a new phase of movement. Indeed, the resulting boulders were moved inland separately from the WCP to the current position on the SB just after having been broken during a successive storm impact. Bioindicators and morphological

**Table 3**
Dimensional parameters of the boulders.*The boulder volume was calculated by means of a laser scanner software.

| | a axis (m) | b axis (m) | c axis (m) | Volume* ($m^3$) | $\gamma_d$ ($g/cm^3$) | Weight (t) |
|---|---|---|---|---|---|---|
| Boulder A | 3,60 | 2,60 | 0,38 | 6,90 | 2,3 | 15,87 |
| Boulder B | 2,60 | 2,10 | 1,10 | 3,85 | 2,3 | 8,86 |
| Boulder C | 6,20 | 2,60 | 0,38 | 10,75 | 2,3 | 24,73 |

Please cite this article in press as: Piscitelli, A., et al., Numerical approach to the study of coastal boulders: The case of Martigues, Marseille, France, Quaternary International (2016), http://dx.doi.org/10.1016/j.quaint.2016.10.042

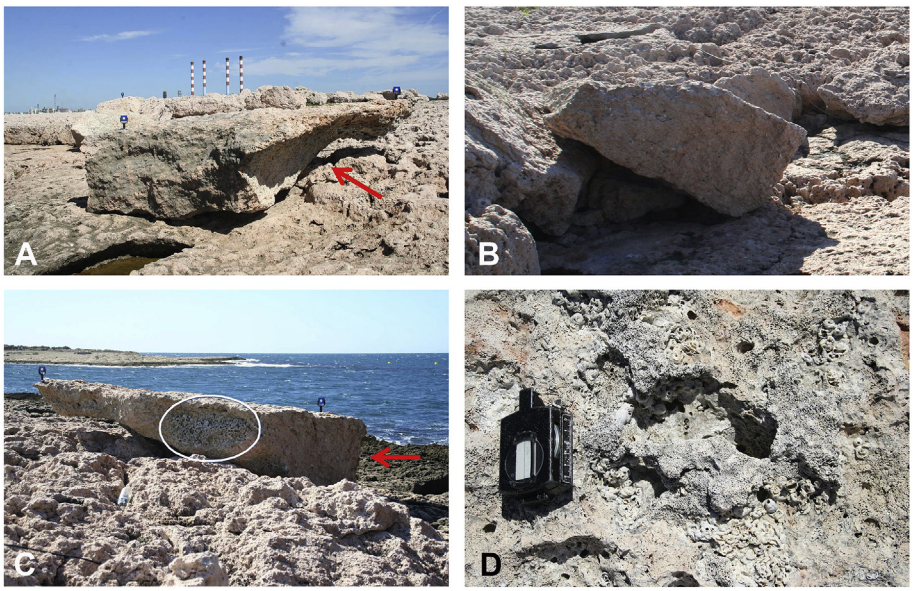


**Fig. 9.** Morphological and biological evidence on the blocks "A" and "B". A: the surface indicated by the arrow represents the original face turned upwards; B: the break surface of block B; C: biological evidence of *Lithophyllum bissoides* rim (white circle) on the block "A" and the break surface indicated by the arrow; D: biological evidence of *Lithophyllum bissoides*, vermetids and barnacles on the upper surface of block "B".

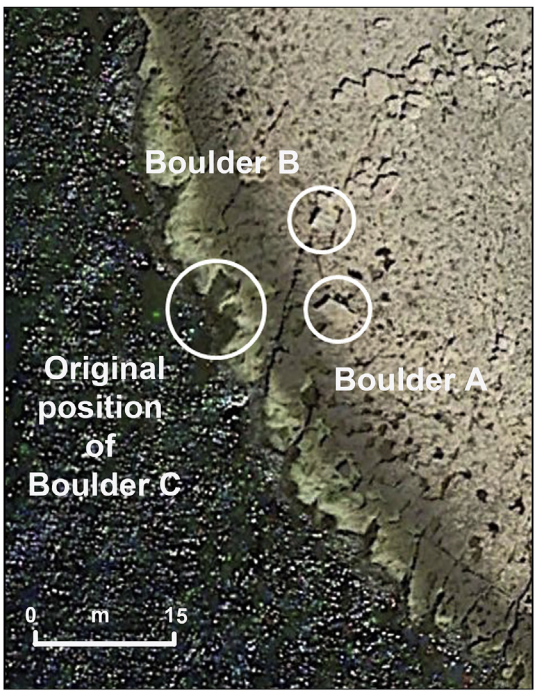


**Fig. 10.** Original position and detachment zone of boulder "C" on the WCP and positions of the blocks "A" and "B" (from Google Earth, December 2003).

aspects, in particular, provide evidence that during the movement, boulder "A" was scattered inland while overturning and, boulder "B" migrated inland, rotating approximately 90Åã anticlockwise (Fig. 11).

### 5.2. Hydrodynamic calculations

The data set can be analyzed to prove this sequence of morpho-events by also using a numerical approach. In this way, it is possible to define a morphodynamic sequence recognizable in a morpho-sequence, although specific dates are not available. The wave features responsible for the initial detachment and inland transport of these two boulders can be determined by applying the Pignatelli et al. (2009) hydrodynamic equations, considering the possible scenarios (Nott, 1997, 2003) that characterized the previous history as: ì - boulder "C" was in a Joint Bounded Scenario (JBS) at the external border of the SB facing the impacting waves; ìì - the same boulder was disarticulated and then collapsed onto the WCP, but remained there in its integrity; ìîì -, the two parts into which boulder "C" broke moved separately, but perhaps simultaneously from the WCP to SB due to waves impacting in a Sub-aerial Boulder Scenario (SBS). Apparently, this does not seem to be the right scenario; indeed, after the collapse, during the phase ìì and ìîì, boulder "C" was below sea level during a wave absence, but alternately in an emerged and submerged position in function of the breaking wave features during the storm. As a consequence, due to the low water level of the wave-cut platform, and the behavior and impacting waves of a strong storm on a WCP, an SBS was considered in order to explain the movement that split boulder "C" into "A" and "B", and, finally deposited both on the surf bench. Assuming these aspects when applying the Pignatelli et al. (2009) equation, possible wave heights (Hs) were estimated:

- **JBS** for Boulder "C" $H_s = (2*c*(\gamma_d-\gamma_w)/\gamma_w)/C_l$
- **SBS** for both Blocks "A" and "B" $H_s = (2*(b*(\gamma_d-\gamma_w)/\gamma_w-2*(C_i*u_i)/g))/((b/c)*C_l+(c/b)*C_d)$

Please cite this article in press as: Piscitelli, A., et al., Numerical approach to the study of coastal boulders: The case of Martigues, Marseille, France, Quaternary International (2016), http://dx.doi.org/10.1016/j.quaint.2016.10.042

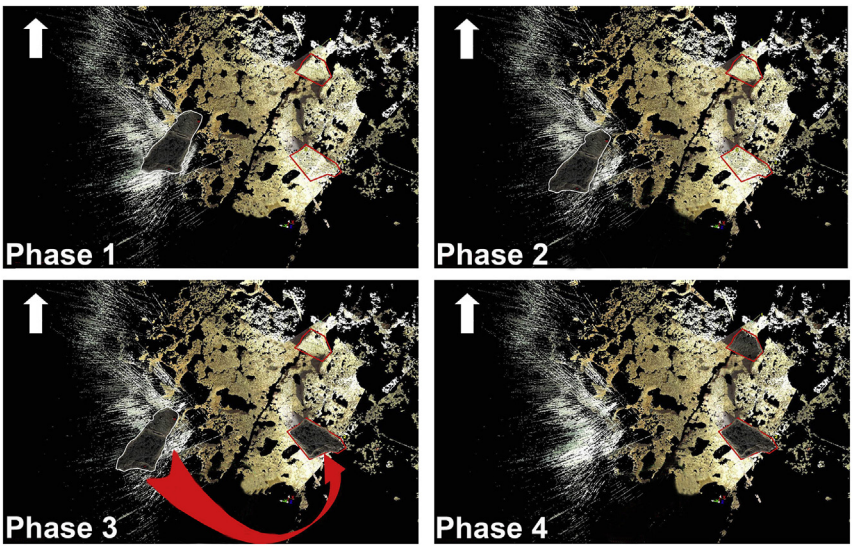


**Fig. 11.** Reconstruction of the succession of events. Phase 1: boulder "C" is in a Joint Bounded Scenario (JBS); Phase 2: boulder "C" is detached and placed on the WCP; Phase 3: the block "A" moves inland while turning in a clockwise direction and overturns; Phase 4: the block "B" moves inward while turning of approximately 90° counter-clockwise.

where $H_s$ is the storm wave height at breaking point, *c* is the minor axis, *b* is the medium axis, $\gamma_d$ is the boulder density, $\gamma_w$ is the water density, $C_l$ is the lift coefficient (Einstein and El Samni, 1949), $C_d$ is the drag coefficient (Helley, 1969), $C_i$ is the inertia coefficient (Noji et al., 1985), *g* is the gravity constant and $u_i$ is the instant acceleration wave (Nott, 1997, 2003).

Other hydrodynamic models were tested in order to compare the possible resulting values of wave heights (Table 5). We applied formulas by:

a Engel and May (2012) (*V* is the volume, *a* is the major axis, $\alpha$ is the slope of the coast, and *q* is an empirical volume coefficient):

- **JBS** for Boulder "C" $\mathbf{H_s}= 2*(\gamma_d-\gamma_w)*V*(\cos\alpha+u_i*\sin\alpha)/(\gamma_w*C_l*a*b*q)$
- **SBS Rampart** for both Blocks "A" and "B" $\mathbf{H_s}= 2*u_f*V*\gamma_d/(\gamma_w*C_d*a*c*q)$

b Nandasena et al. (2011), ($u_s$ is the static friction coefficient):

- **JBS** for Boulder "C" $\mathbf{H} = [(2*(\gamma_d/\gamma_w-1)*g*c*(\cos\alpha+u_s*\sin\alpha)]/C_l$
- **SBS Sliding** for Block "B" $\mathbf{H} = [(2*(\gamma_d/\gamma_w-1)*g*c*(u_i*\cos\alpha+\sin\alpha))/(C_d*(c/b)+u_sC_l)]/\delta g$
- **SBS Overturning** for Block "A" $\mathbf{H} = [2*(\gamma d/\gamma w-1)*g*c*(\cos\alpha+(c/b)*\sin\alpha)]/[Cd*(c^2/b^2)+Cl]/\delta g$

c Benner et al. (2010) ($C_m$ is the inertia coefficient):

$\mathbf{H_s}= 2*b*c*[(\gamma_d-\gamma_w/\gamma_w)*b-(\gamma_d/\gamma_w)*C_m*(u_i/g)*c]/(C_d*c^2+C_l*b^2)$

The minimum wave heights needed to detach the original boulder "C" from the upper part of the wave-cut platform in a JBS, and move boulders "A" and "B" separately from the wave-cut platform to the surf bench in SBS, were calculated. The results of all hydrodynamic equations are shown in Table 4. Many authors have used Nott's derived equations to determine if sea storm or tsunamis were responsible for boulder displacement (i.e. Mastronuzzi and Sansò, 2004; Scicchitano et al., 2007; Maouche et al., 2009); generally, these studies are affected by an overestimation in the calculated wave heights as results of both (ì) approximation typical of the techniques of measurement (Marsico et al., 2009; Hoffmeister et al., 2014) and (ìì) hydrodynamic equations (i.e. Paris et al., 2009; Goto et al., 2010; Bourgeois and MacInnes, 2010). Different models derived by experiments in

**Table 4**
Storm wave Hs obtained by different hydrodynamic equations for boulders A, B and C.

| | Engel and May (2012) | Nandasena et al (2011) | Benner et al. (2010) | Pignatelli et al (2009) |
|---|---|---|---|---|
| | Hs (m) | H (m) | Hs (m) | Hs (m) |
| Boulder A (SBS) | 6,35 | 4,58 | 6,25 | 3,97 |
| Boulder B (SBS) | 4,89 | 3,10 | 5,53 | 3,66 |
| Boulder C (JBS) | 5,72 | 5,61 | 6,25 | 5,36 |

Please cite this article in press as: Piscitelli, A., et al., Numerical approach to the study of coastal boulders: The case of Martigues, Marseille, France, Quaternary International (2016), http://dx.doi.org/10.1016/j.quaint.2016.10.042

**Table 5**
Number of events with height > 3 m and the highest waves selected per 10° range direction recorded in the period 1993–2008.

| Wave range direction | Observed Period 1993–2008 | |
|---|---|---|
| | N. events with H > 3 m | Highest wave in m |
| 150-160 °N | 14 | 4,38 |
| 160-170 °N | 11 | 4,35 |
| 170-180 °N | 18 | 5,48 |
| 180-190 °N | 45 | 5,16 |
| 190-200 °N | 90 | 5,15 |
| 200-210 °N | 19 | 5,25 |
| 210-220 °N | 0 | // |
| 220-230 °N | 0 | // |
| 230-240 °N | 0 | // |
| 240-250 °N | 0 | // |
| 250-260 °N | 0 | // |
| 260-270 °N | 1 | 3,23 |
| 270-280 °N | 17 | 4,15 |
| 280-290 °N | 38 | 4,17 |
| 290-300 °N | 83 | 4,34 |
| **TOTAL** | **336** | |

flume provide a theoretical approach in which morphological and dynamic approximations are adopted on a reduced scale, aimed to reproduce the reality of an impacting wave (articulation of coastline, bathymetry and topography; variety of the rocky coast type, presence of a roughness coefficient, wave direction, etc.) (Imamura et al., 2008; Matsutomi and Okamoto, 2010). On the other hand, the use of Nott's derived equations is, at present, the only way to obtain a deterministic approach which allows the use of "real" data deriving from the observation of a "real" sediment and/or form. Despite this, however, it is evident that among the considered equations two (Benner et al., 2010; Engel and May 2012) provide very high values; the other two (Nandasena et al., 2011; Pignatelli et al., 2009) supply results, which, albeit not absolutely fitting, are surely more compatible, differing by no more than about 0.40–0.50 m for both considered scenarios.

### 5.3. Wave analysis

Having considered the orientation of the coastline and the

**Table 6**
Hydrodynamic parameters of the events with an $H_b$ prox to the minimum value ($H_b$ > 3,66 m) useful to move boulders A and B. $H_0$ = Wave Height offshore; $L_0$ = Wave Length offshore; $W_d$ = Water Depth at breaking point; $H_b$ = Wave Height at breaking point.

| Date | Wave height H (m) | Wave direction (°N) | Period (s) | Wave length $L_0$(m) | Breaking water depth $W_d$ (m) | Breaking wave height $H_b$(m) |
|---|---|---|---|---|---|---|
| 06/01/1994 | 3,85 | 193 | 8,36 | 109,06 | 4,61 | 3,44 |
| 06/01/1994 | 4,24 | 193 | 8,49 | 112,48 | 5,00 | 3,73 |
| 06/01/1994 | 4,62 | 192 | 8,95 | 125,00 | 5,47 | 4,08 |
| 06/01/1994 | 4,73 | 193 | 8,68 | 117,57 | 5,49 | 4,09 |
| 06/01/1994 | 4,70 | 190 | 8,97 | 125,56 | 5,55 | 4,14 |
| 06/01/1994 | 4,87 | 188 | 8,96 | 125,28 | 5,70 | 4,25 |
| 07/01/1994 | 3,71 | 197 | 9,11 | 129,51 | 4,68 | 3,49 |
| 07/01/1994 | 4,47 | 197 | 9,12 | 129,79 | 5,39 | 4,02 |
| 07/01/1994 | 4,66 | 193 | 9,05 | 127,81 | 5,54 | 4,13 |
| 23/01/1996 | 4,04 | 159 | 7,97 | 99,12 | 4,67 | 3,48 |
| 23/01/1996 | 4,38 | 152 | 8,23 | 105,70 | 5,04 | 3,76 |
| 11/11/1996 | 4,17 | 182 | 7,77 | 94,21 | 4,72 | 3,52 |
| 11/11/1996 | 4,46 | 185 | 8,25 | 106,21 | 5,12 | 3,82 |
| 11/11/1996 | 4,77 | 187 | 8,43 | 110,90 | 5,44 | 4,06 |
| 12/11/1996 | 3,66 | 185 | 8,29 | 107,24 | 4,42 | 3,30 |
| 12/11/1996 | 3,98 | 186 | 8,41 | 110,37 | 4,74 | 3,54 |
| 12/11/1996 | 4,33 | 186 | 8,58 | 114,88 | 5,10 | 3,81 |
| 12/11/1996 | 4,66 | 190 | 8,86 | 122,50 | 5,48 | 4,09 |
| 12/11/1996 | 4,95 | 190 | 8,99 | 126,12 | 5,78 | 4,31 |
| 12/11/1996 | 5,11 | 188 | 8,63 | 116,22 | 5,80 | 4,32 |
| 12/11/1996 | 5,16 | 190 | 8,98 | 125,84 | 5,96 | 4,44 |
| 03/01/1997 | 4,25 | 178 | 7,86 | 96,41 | 4,82 | 3,59 |
| 03/01/1997 | 4,35 | 190 | 8,38 | 109,59 | 5,06 | 3,78 |
| 04/01/1997 | 3,76 | 196 | 8,91 | 123,89 | 4,68 | 3,49 |
| 04/01/1997 | 4,19 | 195 | 8,55 | 114,08 | 4,97 | 3,71 |
| 06/11/1997 | 4,55 | 176 | 7,98 | 99,37 | 5,11 | 3,81 |
| 06/11/1997 | 5,19 | 174 | 8,51 | 113,01 | 5,82 | 4,34 |
| 06/11/1997 | 5,48 | 173 | 9,17 | 131,22 | 6,30 | 4,70 |
| 06/11/1997 | 5,43 | 180 | 9,34 | 136,13 | 6,31 | 4,71 |
| 07/11/1997 | 3,47 | 191 | 9,4 | 137,89 | 4,53 | 3,37 |
| 07/11/1997 | 4,32 | 189 | 9,64 | 145,02 | 5,40 | 4,03 |
| 07/11/1997 | 5,07 | 187 | 9,54 | 142,04 | 6,06 | 4,52 |
| 18/12/1997 | 3,91 | 165 | 7,53 | 88,48 | 4,43 | 3,30 |
| 18/12/1997 | 4,07 | 159 | 7,57 | 89,42 | 4,58 | 3,41 |
| 18/12/1997 | 4,16 | 156 | 7,59 | 89,90 | 4,66 | 3,47 |
| 18/12/1997 | 4,24 | 155 | 7,63 | 90,85 | 4,74 | 3,53 |
| 18/12/1997 | 4,41 | 156 | 7,75 | 93,73 | 4,92 | 3,67 |
| 18/12/1997 | 4,35 | 161 | 7,96 | 98,88 | 4,93 | 3,68 |
| 24/10/1999 | 3,84 | 200 | 8,23 | 105,70 | 4,57 | 3,41 |
| 24/10/1999 | 4,03 | 199 | 8,33 | 108,28 | 4,77 | 3,55 |
| 24/10/1999 | 4,01 | 198 | 8,38 | 109,59 | 4,76 | 3,55 |
| 25/10/1999 | 3,69 | 198 | 8,35 | 108,80 | 4,47 | 3,33 |
| 28/12/1999 | 4,07 | 294 | 7,07 | 78,00 | 4,42 | 3,30 |
| 06/11/2000 | 3,91 | 198 | 7,63 | 90,85 | 4,46 | 3,33 |
| 06/11/2000 | 3,74 | 199 | 8,45 | 111,42 | 4,54 | 3,38 |
| 06/11/2000 | 4,07 | 198 | 8,13 | 103,14 | 4,74 | 3,54 |
| 02/03/2001 | 4,37 | 203 | 8,52 | 113,28 | 5,12 | 3,82 |
| 03/03/2001 | 3,52 | 201 | 9,33 | 135,84 | 4,56 | 3,40 |

Please cite this article in press as: Piscitelli, A., et al., Numerical approach to the study of coastal boulders: The case of Martigues, Marseille, France, Quaternary International (2016), http://dx.doi.org/10.1016/j.quaint.2016.10.042

**Table 6** (*continued*)

| Date | Wave height H (m) | Wave direction (°N) | Period (s) | Wave length $L_0$(m) | Breaking water depth $W_d$ (m) | Breaking wave height $H_b$(m) |
|---|---|---|---|---|---|---|
| 03/03/2001 | 4,11 | 201 | 9,30 | 134,97 | 5,11 | 3,81 |
| 03/03/2001 | 4,66 | 203 | 9,19 | 131,79 | 5,58 | 4,16 |
| 31/10/2003 | 4,35 | 199 | 8,35 | 108,80 | 5,05 | 3,77 |
| 31/10/2003 | 4,58 | 201 | 9,42 | 138,47 | 5,58 | 4,16 |
| 31/10/2003 | 5,00 | 202 | 8,73 | 118,93 | 5,74 | 4,28 |
| 31/10/2003 | 5,05 | 201 | 9,32 | 135,55 | 5,97 | 4,45 |
| 31/10/2003 | 5,25 | 202 | 9,22 | 132,66 | 6,12 | 4,56 |
| 01/11/2003 | 3,94 | 198 | 9,54 | 142,02 | 5,02 | 3,74 |
| 18/01/2005 | 3,90 | 298 | 7,70 | 92,52 | 4,47 | 3,33 |
| 19/01/2005 | 4,05 | 299 | 8,20 | 104,93 | 4,75 | 3,54 |
| 02/12/2005 | 3,77 | 194 | 10,30 | 165,55 | 5,05 | 3,76 |
| 02/12/2005 | 4,52 | 197 | 9,00 | 126,40 | 5,40 | 4,03 |
| 02/12/2005 | 4,53 | 195 | 10,10 | 159,19 | 5,73 | 4,27 |
| 02/12/2005 | 5,15 | 200 | 9,60 | 143,82 | 6,15 | 4,59 |
| 02/12/2005 | 5,03 | 196 | 10,10 | 159,19 | 6,20 | 4,62 |
| 19/02/2006 | 3,67 | 198 | 9,20 | 132,08 | 4,67 | 3,48 |
| 19/02/2006 | 3,95 | 196 | 8,50 | 112,75 | 4,74 | 3,54 |
| 19/02/2006 | 4,09 | 198 | 9,10 | 129,23 | 5,04 | 3,76 |
| 19/02/2006 | 4,30 | 197 | 9,00 | 126,40 | 5,20 | 3,88 |
| 04/03/2006 | 3,56 | 206 | 8,90 | 123,61 | 4,49 | 3,35 |
| 04/03/2006 | 3,60 | 200 | 9,30 | 134,97 | 4,63 | 3,45 |
| 23/01/2007 | 4,08 | 281 | 8,30 | 107,50 | 4,80 | 3,58 |
| 23/01/2007 | 4,17 | 285 | 8,40 | 110,11 | 4,91 | 3,66 |
| 24/01/2007 | 3,84 | 291 | 8,20 | 104,93 | 4,56 | 3,40 |
| 24/01/2007 | 3,86 | 291 | 8,30 | 107,50 | 4,61 | 3,43 |
| 24/01/2007 | 3,91 | 290 | 8,20 | 104,93 | 4,62 | 3,45 |
| 24/01/2007 | 4,13 | 288 | 8,30 | 107,50 | 4,85 | 3,61 |
| 24/01/2007 | 4,09 | 290 | 8,40 | 110,11 | 4,84 | 3,61 |
| 28/05/2007 | 4,00 | 287 | 8,20 | 104,93 | 4,70 | 3,50 |
| 28/05/2007 | 4,16 | 300 | 8,30 | 107,50 | 4,87 | 3,63 |
| 28/05/2007 | 4,34 | 296 | 8,30 | 107,50 | 5,03 | 3,75 |
| 29/05/2007 | 3,93 | 297 | 8,10 | 112,39 | 4,61 | 3,44 |
| 09/12/2007 | 3,99 | 279 | 8,20 | 104,93 | 4,69 | 3,50 |
| 10/12/2007 | 3,75 | 283 | 8,20 | 104,93 | 4,48 | 3,34 |
| 10/12/2007 | 3,93 | 282 | 8,30 | 107,50 | 4,67 | 3,48 |
| 10/12/2007 | 4,01 | 279 | 8,30 | 107,50 | 4,74 | 3,53 |
| 10/12/2007 | 4,15 | 280 | 8,40 | 110,11 | 4,89 | 3,65 |
| 10/12/2007 | 4,17 | 281 | 8,40 | 110,11 | 4,91 | 3,66 |
| 11/01/2008 | 3,87 | 202 | 8,30 | 107,50 | 4,61 | 3,44 |
| 21/03/2008 | 3,97 | 277 | 7,80 | 94,94 | 4,56 | 3,40 |
| 20/04/2008 | 3,83 | 168 | 8,30 | 107,50 | 4,63 | 3,45 |
| 21/11/2008 | 4,04 | 300 | 8,20 | 104,93 | 4,74 | 3,53 |
| 21/11/2008 | 4,19 | 300 | 8,40 | 110,11 | 4,93 | 3,67 |
| 29/11/2008 | 4,13 | 196 | 9,50 | 140,84 | 5,18 | 3,87 |
| 29/11/2008 | 4,51 | 195 | 9,00 | 126,40 | 5,39 | 4,02 |

present position of the boulders, the direction of storm waves needed to move boulders "A" and "B" was evaluated to be approximately 225°N ± 15°. During the period 1993–2008, the buoy in the Gulf of Lion indicated an occurrence of waves coming from the 150°N-300°N directions, about 1500 of which were over 3 m high, and about 340 with the same wave height. Only storm waves with H > 3 m and 150°N-300°N directions were considered (Table 5). Storm waves that have offshore directions between N150E and N300E, and an 0°–75° incidence range, reach the shoreline with incidence angles ranging 2°–8° (i.e.: A.S.C.E., 1974 and references therein).

From its breaking point to the coastline, the wave height first decreases slightly and then greatly increases in the last 3 m due to the sea floor trend. Indeed, the sudden slope increasing of the seabed amplifies the shoaling process, so that the wave height near the coastline becomes very close to the $H_b$ value (i.e.: Keulegan and Paterson, 1940; Sunamura and Horikawa, 1974). As shown in Table 5, according to the Pignatelli et al. hydrodynamic model (2009), a minimum wave height of 5.36 m is required to detach boulder "C" in a JBS; while, to move boulders "A" and "B" from the wave-cut platform inland, minimum wave heights, respectively, of 3.97 and 3.66 m are required in an SBS. Among the recorded waves with H > 3 m, at their breaking point, 47 waves present wave heights ($H_b$) ≥ 3.66 m (Sunamura, 1992) and water depths ($W_d$) between 4.91 and 6.31 m (Keulegan and Patterson, 1940). On the other hand, 26 waves show, at their breaking point, wave heights ($H_b$) ≥ 3.97 m and water depths ($W_d$) between 5.39 and 6.31 m. The wave direction of all these events is between N152E and N285E. All the hydrodynamic parameters/features of the above-mentioned waves are shown in Table 6. By analysing satellite photos available as of December 2003, it was already possible to observe and locate the presence of boulders "A" and "B" on the surf bench. Thus, only storm waves occurring before that date can be considered responsible for detaching and subsequently displacing the boulders. The hydrodynamic parameters related to the surveyed sea floor trend as well as the accounts of eyewitnesses are absolutely compatible with the minimum Hs values of the Pignatelli et al. (2009) and Nandasena et al. (2011) models for both Joint Bounded and Sub-aerial Boulder scenarios.

## 6. Conclusions

The presence of boulders on the SB whose positions, thanks to eyewitness, are ascribed to the impact of a strong storm occurring in the last two decades, warrants the possibility to test the validity of the hydrodynamic model in a real case study the cause of which

Please cite this article in press as: Piscitelli, A., et al., Numerical approach to the study of coastal boulders: The case of Martigues, Marseille, France, Quaternary International (2016), http://dx.doi.org/10.1016/j.quaint.2016.10.042

is known: the impact of storm waves. The use of digital survey technologies – TLS and DGPS - coupled with a traditional geomorphological survey and the use of hydrodynamic equations have allowed to study boulder movement in coastal scenarios using a quantitative–mathematical approach.

The history of the studied boulders was reconstructed on the basis of a 3D survey and the presence of bio-encrustations that allowed an estimate of the future position of boulder "C" situated in JBS at the external limit of the SB, exposed to the impact of waves. With the same approach, it was possible to estimate the phase during which boulder "C" completely collapsed into the water onto the WCP establishing permanent position submerged during calm waters. In the JBS, the application of different hydrodynamic equations suggests that a storm wave of about minimum 5.5 m high was required to move boulder "C" from the coast, according to the Pignatelli et al. (2009) and of Nandasena et al. (2011) models. An analysis of the wave climate history of the sea lapping the studied area suggests that this value is consistent with very energetic storms.

According to the satellite images, in a subsequent phase, prior to December 2003, the boulder was eventually split into two parts, becoming boulders "A" and "B". Just after this and during the same storm, the two boulders were separately transported inland by storm waves from the wave-cut platform to their present positions on the surf bench, as evidenced by both the bio-indicators and the morphological aspects highlighted by the digital survey and by the 3D view. In this case, two hydrodynamic models, Pignatelli et al. (2009) and Nandasena et al. (2011), suggest a wave of 3.5–4 m high capable of moving boulders inland, versus other models that establish a wave height of more than 6.3 m; the first values are in agreement with "the normal very energetic storms" that characterise the studied area.

To conclude, it was not necessary to have a tsunami impact, which among other things has never been recorded in the past 20 years, to move boulders "A" and "B" inland; these movements occurred before December 2003.

The hydrodynamic parameters of 47 waves (selected in the period between 1993 and 2008), in relation to the surveyed sea floor trend and eyewitness accounts, confirm the best fitting of the Pignatelli et al. (2009) and Nandasena et al. (2011) hydrodynamic models with this reconstructed succession of events.

## Acknowledgments

This work has been partially carried out thanks to the support of the Labex OT-Med (n° ANR-11-LABX-0061) and of the AMIDEX (n° ANR-11-IDEX-0001-02) projects, funded by the "Investissements d'Avenir" French Government programme, managed by the French National Research Agency (ANR) and the Flagship Project RITMARE - Italian Research for the Sea - coordinated by the Italian National Research Council and funded by the Italian Ministry of Education, University and Research within the National Research Programme 2011–2013, and by the PRIN 2010/2011 "*Response of morphoclimatic system dynamics to global changes and related geomorphological hazard*".

This paper is a French- Italian contribution to the project IGCP 639–International Geological Correlation Programme "Sea-level change from minutes to millennia" by UNESCO – IUGS (Project Leaders: S. Engelhart, G. Hoffmann, F. Yu and A. Rosentau).

We would like to thank Ms. Patricia Salomone and Prof. Vicky Sportelli for having improved the English form, and two anonymous referees that offered very valid suggestions to greatly improve the entire manuscript.

## References

Anzidei, M., Antonioli, F., Furlani, S., Lambeck, K., Mastronuzzi, G., Serpelloni, E., Vannucci, G., 2014. Coastal structure, sea level changes and vertical motion of the land in the Mediterranean. In: Martini, I.P., Wanless, H.R. (Eds.), Sedimentary Coastal Zones from High to Low Latitudes: Similarities and Differences. Geological Society, London, Special Publications, p. 388.

Barbano, M.S., Pirrotta, C., Gerardi, F., 2010. Large boulders along the southeastern Ionian coast of Sicily: storm or tsunami deposits? Mar. Geol. 275, 140–154.

Benner, R., Browne, T., Brückner, H., Kelletat, D., Scheffers, A., 2010. Boulder transport by waves: progress in physical modeling. Z. Geomorphol. 54 (3), 127–146.

Biolchi, S., Furlani, S., Antonioli, F., Baldassini, N., Causon Deguara, J., Devoto, S., Di Stefano, A., Evans, J., Gambin, T., Gauci, R., Mastronuzzi, G., Monaco, C., Scicchitano, G., 2016. Boulder accumulations related to extreme wave events on the eastern coast of Malta. Nat. Hazards Earth Syst. Sci. 16, 737–756.

Bourgeois, J., MacInnes, B., 2010. Tsunami boulder transport and other dramatic effects ofthe 15 November 2006 central Kuril Islands tsunami on the island of Matua. Z. Geomorphol. 54 (3), 175–195.

Colomb, E., Rouire, J., L'Homer, A., 1975. Geological Map of the France, Map of Istres. Map 1019, Scale 1:50,000 (Bur. de Rech. Geol. et Min., Orléans, France).

Einstein, H.A., El Samni, E.A., 1949. Hydrodynamic forces on a rough wall. Rev. Mod. Phys. 21–3, 520–524.

Engel, M., May, S.M., 2012. Bonaire's boulder fields revisited evidence for Holocene tsunami impact on the Leeward Antilles. Quat. Sci. Rev. 54, 126–141.

Goto, K., Chavanich, S.A., Imamura, F., Kunthasap, P., Matsui, T., Minoura, K., Sugawara, D., Yanagisawa, H., 2007. Distribution, origin and transport process of boulders deposited by the 2004 Indian Ocean tsunami at Pakarang Cape, Thailand. Sediment. Geol. 202, 821–837.

Goto, K., Miyagi, K., Kawamata, H., Imamura, F., 2010. Discrimination of boulders deposited by tsunamis and storm waves at Ishigaki Island, Japan. Mar. Geol. 269, 34–45.

Helley, E.J., 1969. Field measurement of the initiation of large bed particle motion in blue creek near Klamath, California. In: U.S. Geological Survey Professional Paper, 562-G, p. 19.

Hippolyte, J.-C., Angelier, J., Nury, D., Bergerat, F., Guieu, G., 1993. Tectonic-stratigraphic record of paleostress time changes in the Oligocene basins of the Provence, southern France. Tectonophysics 226, 15–35.

Hoffmeister, D., Ntageretzis, K., Aasen, H., Curdt, C., Hadler, H., Willershäuser, T., Bareth, G., Brückner, H., Vött, A., 2014. 3D model-based estimations of volume and mass of high-energy dislocated boulders in coastal areas of Greece by terrestrial laser scanning. Z. Geomorphol. 58 (3), 115–135.

Imamura, F., Goto, K., Ohkubo, S., 2008. A numerical model for the transport of a boulder by tsunami. J. Geophys. Res. 113, C01008.

Jaffe, B., Buckley, M., Richmond, B., Strotz, L., Etienne, S., Clark, K., Watt, S., Gelfenbaum, G., Goff, J., 2011. Flow speed estimated by inverse modeling of sandy sediment deposited by the 29 September 2009 tsunami near Satitoa, east Upolu, Samoa. Earth Sci. Rev. 107, 23–37.

Jaffe, B.E., Goto, K., Sugawara, D., Richmond, B.M., Fujino, S., Nishimura, Y., 2012. Flow speed estimated by inverse modeling of the sandy tsunami deposit: results from 11 March 2011 tsunami on the coastal plain near the Sendai Airport, Honshu, Japan. Sediment. Geol. 282, 90–109.

Jolivet, L., Prouteau, G., Brun, J.P., Meyer, B., Rouchy, J.M., Scaillet, B., 2008. Géodynamique Méditerranéenne. Vuibert-SGS, p. 232.

Julian, M., Anthony, E.J., 1996. Aspects of landslide activity in the mercantour massif and the French Riviera, south eastern France. Geomorphology 15, 275–289.

Kaniewski, N., Marriner, N., Morhange, C., Faivre, S., Otto, T., Van Campo, E., 2016. Solar pacing of storm surges, coastal flooding and agricultural losses in the Central Mediterranean. Nat. Sci. Rep. 6, 25197.

Keulegan, G., Patterson, G.W., 1940. Mathematical theory of irrotational translation waves. J. Res. Natl. Bureau Stand. 24, 47–101.

Laborel, J., Laborel-Deguen, F., 1994. Biological indicators of relative sea-level variations and of co-seismic displacements in the Mediterranean region. J. Coast. Res. 10 (2), 395–415.

Maouche, S., Morhange, C., Meghraoui, M., 2009. Large boulder accumulation on the Algerian coast. Evidence of catastrophic tsunami events in the Western Mediterranean. Mar. Geol. 206, 96–104.

Marsico, A., Pignatelli, C., Piscitelli, A., Mastronuzzi, G., Pennetta, L., 2009. Ricostruzione digitale di blocchi accumulati da eventi estremi in Italia meridionale. In: Atti 13ª Conferenza Nazionale ASITA, 1–4 Dicembre 2009, pp. 1377–1385.

Mastronuzzi, G., Brückner, H., De Martini, P.M., Regnauld, H., 2013. Tsunami: from the open sea to the coastal zone and beyond. In: Mambretti, S. (Ed.), Tsunami: from Fundamentals to Damage Mitigation. WIT Press, Southampton, pp. 1–36.

Mastronuzzi, G., Pignatelli, C., 2012. The boulders berm of Punta Saguerra (Taranto, Italy): a morphological imprint of 4th april, 1836 Rossano Calabro tsunami? Earth Planets Space 64 (10), 829–842.

Mastronuzzi, G., Pignatelli, C., Sansò, P., 2006. Boulder fields: a valuable morphological indicator of paleotsunami in the Mediterranean Sea. Z. Geomorphol. N.F. Suppl. Bd 146, 173–194.

Mastronuzzi, G., Pignatelli, C., Sansò, P., Selleri, G., 2007. Boulder accumulations produced by the 20th February 1743 tsunami along the coast of southeastern Salento (Apulia region, Italy). Mar. Geol. 242, 191–205.

Mastronuzzi, G., Sansò, P., 2000. Boulders transport by catastrophic waves along the Ionian coast of Apulia (Southern Italy). Mar. Geol. 170, 93–103.

Mastronuzzi, G., Sansò, P., 2004. Large boulder accumulations by extreme waves

Please cite this article in press as: Piscitelli, A., et al., Numerical approach to the study of coastal boulders: The case of Martigues, Marseille, France, Quaternary International (2016), http://dx.doi.org/10.1016/j.quaint.2016.10.042

along the adriatic coast of southern apulia (Italy). Quat. Int. 120, 173–184.
Matsutomi, H., Okamoto, K., 2010. Inundation flow velocity of tsunami on land. Isl. Arc 19, 443–457.
Morhange, C., Marriner, N., 2015. Archeological and biological relative sea-level indicators. In: Shennan, I., Long, A.J., Horton, B.P. (Eds.), Handbook of Sea Level Research. Wiley, pp. 146–156.
Morhange, C., Marriner, N., Pirazzoli, A., 2006. Evidence of late-Holocene tsunami events in Libanon. Z. Geomorphol. 146, 81–95.
Nandasena, N.A.K., Paris, R., Tanaka, N., 2011. Reassessment of hydrodynamic equations: minimum flow velocity to initiate boulder transport by high energy events (storms, tsunamis). Mar. Geol. 281, 70–84.
Noji, M., Imamura, N., Shuto, N., 1985. Numerical simulation of movement of large rocks transported by tsunami. In: Proceedings of the IUGG/IOC International Tsunami Symposium, Wakayama, Japan, pp. 189–197.
Noormets, R., Crook, K.A.W., Felton, E.A., 2004. Sedimentology of rocky shorelines: 3. Hydrodynamics of megaclast emplacement and transport on a shore platform, Oahu, Hawaii. Sediment. Geol. 172, 41–65.
Nott, J., 1997. Extremely high wave deposits inside the great barrier reef, Australia; determining the cause tsunami or tropical cyclone. Mar. Geol. 141, 193–207.
Nott, J., 2003. Waves, coastal boulders and the importance of the pre-transport setting. Earth Planet. Sci. Lett. 210, 269–276.
Paris, R., Wassmer, P., Sartohadi, J., Lavigne, F., Barthomeuf, B., Desgages, E., Grancher, D., Baumert, P., Vaultier, F., Brunstein, D., Gomez, C., 2009. Tsunamis as geomorphic crisis: lessons from the December 26, 2004 tsunami in Lhok Nga, west banda aceh (sumatra, Indonesia). Geomorphology 104, 1–2, 59-72.
Paris, R., Fournier, J., Poizot, E., Etienne, S., Mortin, J., Lavigne, F., Wassmer, P., 2010. Boulder and fine sediment transport and deposition by the 2004 tsunami in Lhok Nga (western Banda Aceh, Sumatra, Indonesia): a coupled offshore-onshore model. Mar. Geol. 268, 43–54.
Pignatelli, C., Sansò, P., Mastronuzzi, G., 2009. Evaluation of tsunami flooding using geomorphologic evidence. Mar. Geol. 260, 6–18.
Regnauld, H., Oszwald, J., Planchon, O., Pignatelli, C., Piscitelli, A., Mastronuzzi, G., Audevard, A., 2010. Polygenic (tsunami and storm) deposits? A case study from Ushant Island, western France. Z. Geomorphol. 54 (3), 197–217.
Richmond, B.M., Watt, S., Buckley, M., Jaffe, B.E., Gelfenbaum, G., Morton, R.A., 2011. Recent storm and tsunami coarse-clast deposit characteristics, southeast Hawaii. Mar. Geol. 283, 1–4.
Scicchitano, G., Monaco, C., Tortorici, L., 2007. Large boulder deposits by tsunami waves along the Ionian coast of south-eastern Sicily (Italy). Mar. Geol. 238, 75–91.
Shah-Hosseini, M., Morhange, C., De Marco, A., Wante, J., Anthony, E.J., Sabatier, F., Mastronuzzi, G., Pignatelli, C., Piscitelli, A., 2013. Coastal boulders in Martigues, French mediterranean: evidence for extreme storm waves during the Little Ice age. Z. Geomorphol. 57, 181–199.
Sunamura, T., 1992. Geomorphology of Rocky Coasts. John Wiley and Sons, p. 302.
Sunamura, T., Horikawa, K., 1974. Two dimensional beach transformationdue to waves, proceedings 14th coastal engineering conference. Am. Civ. Eng. 920–938.
Vella, C., Demory, F., Canut, V., Dussouillez, P., Fleury, T.J., 2011. First evidence of accumulation of mega boulders on the Mediterranean rocky coast of Provence (southern France). Nat. Hazards Earth Syst. Sci. 11, 905–914.
Vella, C., Provansal, M., 2000. Relative sea-level rise and neotectonic events during the last 6500 years on the southern eastern Rhône delta, France. Mar. Geol. 170, 27–39.
Vella, C., Bourcier, M., Provansal, M., 1998. Montée du niveau marin et sédimentation holocène sur la marge orientale du delta du Rhône, Provence, France. Bull. Soc. Geol. Fr. 169, 403–414.
Vött, A., Lang, F., Brückner, H., Gaki-Papanastassiou, K., Maroukian, H., Papanastassiou, D., Giannikos, A., Hadler, H., Handl, M., Ntageretzis, K., Willershäuser, T., Zander, A., 2010. Sedimentological and geoarchaeological evidence of multiple tsunamigenic imprint on the Bay of Palairos- Pogonia (Akarnania, NW Greece). Quat. Int. 242 (1), 213–239.

Please cite this article in press as: Piscitelli, A., et al., Numerical approach to the study of coastal boulders: The case of Martigues, Marseille, France, Quaternary International (2016), http://dx.doi.org/10.1016/j.quaint.2016.10.042